

TENSION MECHANISM DYNAMIC ANALYSIS

The aim of the presented article is to show how to create a mathematical model of the tension mechanism working by a spring motion generation and contacting a rigid body at the end of the motion.

Keywords: Mechanism, analysis, contact force, simulation.

1. Introduction

The first step of the above described task solution was the creation of the mechanism mathematical model assembled from three movable parts and the motion generating spring (Fig. 1).

The second step was the analysis of the forces applied on the mechanism during the workflow.

2. Mechanism Modeling

The mechanism movement is generated by a spring affecting the sliding joint between the mechanism parts labeled 2 and 3 (Fig. 1).

The main problem of the analysis is the moment when the mechanism reaches its end position and contacts the frame rigid body with the part 1 (Fig. 1) because of the contact properties of the contact point.

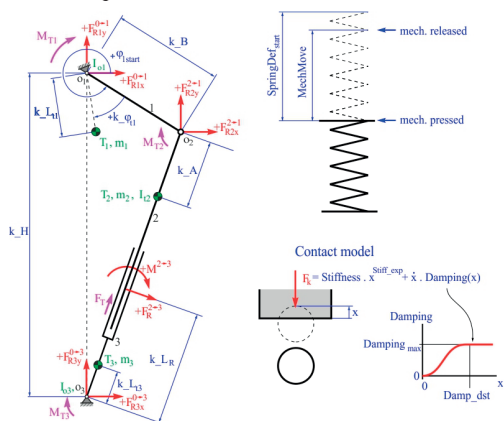


Fig. 1 Model of the mechanism structure including the spring and contact model (Source: authors)

2.1 Dimensions and spring parameters

The kinematics of the mechanism parts parameters were defined according to the 3D model and Table 1.

Dimensions and spring parameters of the mechanism Table 1

Name	Label	Value	Unit
Part 1 length	k_B	0.05	m
Part 1 centre of gravity distance	k_L ₁₁	0.02	m
Part 1 angle of the centre of gravity	k_φ ₁₁	π/4	rad
Part 2 centre of gravity distance	k_A	0.03	m
Part 3 centre of gravity distance	k_L ₁₃	0.02	m
Distance of revolution joints O1 and O3	k_H	0.1	m
Spring stiffness	SpringStiffnes	1000	N.m ⁻¹
Spring working stroke	MechMove	0.03	m
Starting spring deformation	SpringDefstart	0.1	m

The initial values of the mechanism parameters are defined in Table 2.

Initial values of the mechanism parameters Table 2

Name	Label	Value	Unit
Part 1 initial angle of the centre of gravity	φ _{1start}	-π/4	rad
Part 2 initial variable distance	k_L _R	0	m

The angle by the full pressed mechanism is defined as φ_{1start}. The reaction force position k_L_R influences only the moment value M.

* ¹Michal Lukac, ¹Frantisek Brumerick, ¹Leszek Krzywonos, ²Pawel Drozdziel
¹Faculty of Mechanical Engineering University of Zilina, Slovakia
²Mechanical Engineering Faculty, Lublin University of technology, Poland
 E-mail: michal.lukac@fstroj.uniza.sk

The motion generating spring positions are defined in Fig. 2.

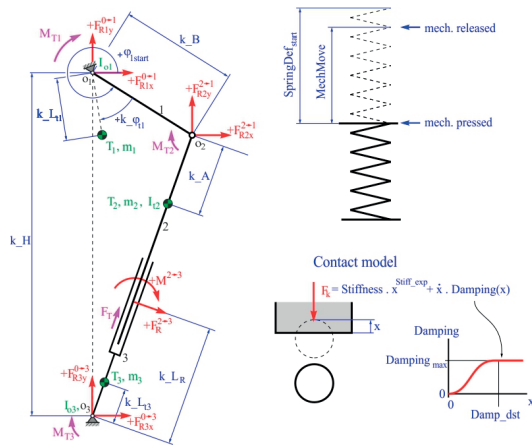


Fig. 2 Spring positions (Source: authors)

2.2 Mass properties

The mechanism mass properties are defined according to the 3D model and its calculation model (Fig. 1) in Table 3.

Mass properties parameters of the mechanism Table 3

Name	Label	Value	Unit
Part 1 mass	m_1	59.238	kg
Part 1 inertia	I_{o1}	$2.843445 \cdot 10^{-2}$	$\text{kg} \cdot \text{m}^2$
Part 2 mass	m_2	0.5	kg
Part 2 inertia	I_{o2}	0.1	$\text{kg} \cdot \text{m}^2$
Part 3 mass	m_3	25.574	kg
Part 3 inertia	I_{o3}	$1.13983182 \cdot 10^{-2}$	$\text{kg} \cdot \text{m}^2$

2.3 Friction and contact properties

The developed simulation program in the chosen software (Mathcad) allows to activate the friction via the created “Friction” GUI button. Contact properties of the mechanism are defined according to the 3D model in Table 4.

Contact properties parameters of the mechanism Table 4

Name	Label	Value	Unit
Mechanism stiffness	Stiffnes	200000	$\text{N} \cdot \text{m}^{-1}$
Stiffness exponent	Stiff_exp	2 ($>=1$)	N.m
Mechanism maximum damping factor	Dampingmax	500	$\text{N} \cdot \text{m}^{-1} \cdot \text{s}$
Distance to max. damping build-up	Damp_dst	0.002	m
Joint O1 friction moment	M_{T1}	0.5	N.m
Joint O1 friction factor	k_{MT1}	0	-
Joint O2 friction moment	M_{T2}	1	N.m
Joint O2 friction factor	k_{MT2}	0	-
Joint O3 friction moment	M_{T3}	1	N.m
Joint O3 friction factor	k_{MT3}	0	-

The $k_{MT1, 2, 3}$ ($\text{rad} \cdot \text{s}^{-1}$) and k_{FT} ($\text{m} \cdot \text{s}^{-1}$) values are considered by the friction button turned to ON. The direction of the friction force (moment) depends on the motion direction (from the motion parts relative velocity sign). If the velocity is too slow, its direction can vary and so can also the direction of the friction force. Therefore, the friction force value is defined to rise around zero velocity to maximum [1] and [2].

The described k-value defines the velocity interval of the maximum friction force. The principle of the calculation is similar to the contact model damping calculation (the value is equivalent to the Damp_dst value). The k-value is different for every friction force because every friction couple velocity varies. The lower is the k-value, the more accurate is the calculation. If the model does not work in the friction mode, the solution is to raise the k-value which is usually $1 \cdot 10^{-3}$ and lower [3]. The k-value does not affect the calculation without the friction consideration. The start of the simulation has to be done with the zero value and the solver type FIXED (parameters for the Mathcad software).

There is also the fcn_step function defined because of the smooth transition between two values of the damping coefficient in the contact point. This leads to smooth rise of this coefficient without the step rise to the maximum in the contact moment.

The value of the damping rises during the defined penetration depth Damp_dst. and then becomes stabilized to “Damping_max” value (Table 4, Fig. 3).

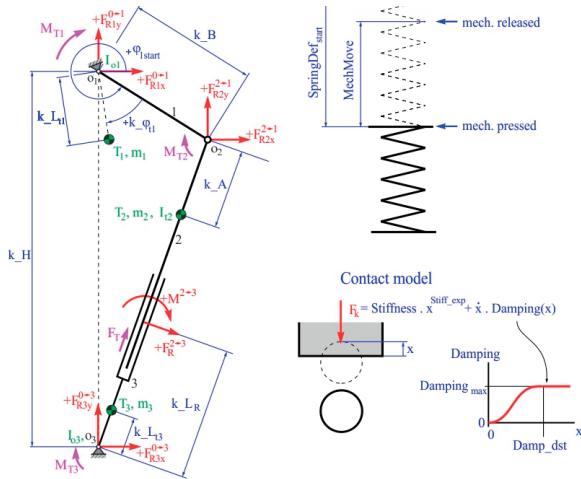


Fig. 3 Contact model (Source: authors)

3. Solver parameters

The solver parameters were defined as follows in Table 5.

Name	Label	Value	Unit
Time interval (0 - t _{end})	t _{count}	1000	-
Number of the points in the plotted graphs	N _t	1001	-
End time of the simulation	t _{end}	1	S
Friction force	F _T	10	N
Friction force factor	k _{FT}	0	-

The larger is the number of the time interval (0 - t_{end}) division during the simulation, the more accurate is the calculation. If the calculation does not converge, new solver has to be used (right button on the odesolve function in the MathCad) [4].

4. Interpolation of bodies coordinates

The bodies coordinates that are interesting for the interpolation during simulation are labeled φ_2 and L_{t2} in Fig. 4. The parameters influencing the interpolation are defined in Table 6.

Name	Label	Value	Unit
Control variable	CTOL	0.00001	-
Control variable	TOL	0.00001	-
Polynomial degree	FitDegree	7	-
Number of points	NuPo	200	-

The Mathcad TOL worksheet variable controls the precision to which integrals and derivatives are evaluated. TOL also controls convergence criteria in Solve Blocks and in the root function. The two most recent estimates of a solution must differ by less than the built-in variable TOL. The CTOL worksheet variable controls how closely a constraint in a Solve Block must be met for a solution to be acceptable. It is used by optimizing functions like: Minimize, Maximize, Find, or Minerr. For example, a constraint such as $x < 2$ must be satisfied to within CTOL before a solution is returned. If CTOL = 0.001 (the default), this constraint is satisfied if $x < 2.001$ [5] and [6].

Figure 4 shows the simplified view of the mechanism with all important variables and their first and second derivatives.

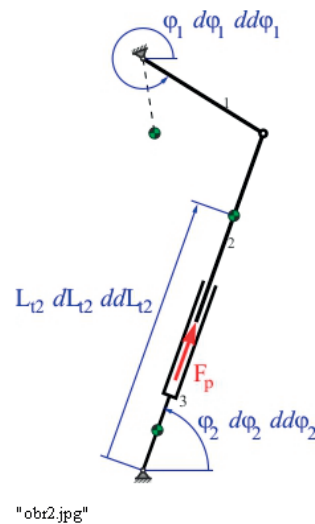


Fig. 4 Simplified view of important mechanism variables (Source: authors)

The calculated mechanism has one degree of freedom (DOF). All forces and masses are reduced to the mechanism part 1 coordinate φ_1 .

It is necessary to define the coordinates L_{t2} and φ_2 as a function of the φ_1 coordinate. To make the calculation effective and simple, the coordinates L_{t2} and φ_2 are defined as a function of the φ_1 by the interpolation polynomial of the 7-th degree! The FitDegree value has to remain defined to 7 during the calculation because all equations are derived for this polynomial degree [7].

The R_disp function displays the L_{t2} and φ_2 coordinate values depending upon φ_1 for the φ_1 values from $-\pi/2$ to $\pi/2$. In this interval, the mechanism is resolvable - the values outside the interval will not be calculated correctly.

The number of values labeled NuPo specifies the calculation of the interpolation polynomial coefficients for the φ_2 and L_{t2} coordinates. The Disp_Coeff software feature displays the polynomial coefficients. The angle of the φ_1 coordinate between the threshold limit $-\pi/2$ and $\pi/2$ is defined as ff1.

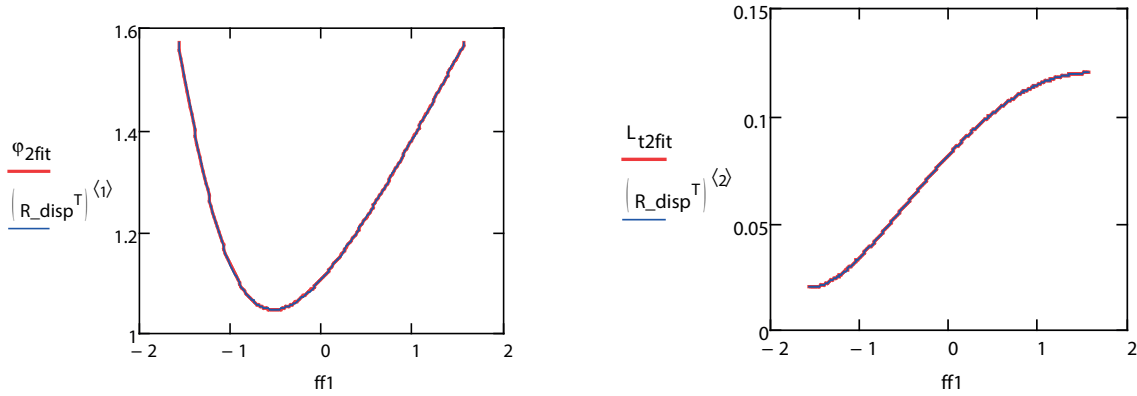


Fig. 5 Interpolated and calculated data match test of the mechanism variables (Source: authors)

The equations representing the relationships between the coordinates are following:

$$\begin{aligned}
 L_{12} \cdot \cos(\varphi_2) + k_A \cdot \cos(\varphi_2) + k_B \cdot \cos(\varphi_1 - \pi) &= 0 \\
 L_{12} \cdot \sin(\varphi_2) + k_A \cdot \sin(\varphi_2) + k_B \cdot \sin(\varphi_1 - \pi) \\
 -k_H &= 0
 \end{aligned} \tag{1}$$

The comparison between the interpolated data (red) and real data (blue) for the angle φ_1 from $-\pi/2$ to $\pi/2$ (Fig. 5) attends only for the test of the interpolated and calculated data match. In the case of extreme mechanism dimensions, the values could not match and it would be necessary to rise the interpolation polynomial degree [8] - [10].

The φ_2 and L_{12} coordinates are defined at the start of the simulation (pressed mechanism) for the value φ_{1start} . The initial values for the calculations noted above are shown in Table 7.

Initial values of the mechanism variables Table 7

Name	Label	Value	Unit
Part 2 initial angle of the centre of gravity	φ_{2start}	61.298	Deg
Part 2 initial variable distance	$L_{12start}$	0.044	M

The spring force labeled as fcn_F_p (def) is defined as linear, the output parameter is the L_{12} value.

5. Motion equation calculation

The differential motion equation for the mechanism is defined according to the labels of the parameters defined in the previous text and tables as

$$\begin{aligned}
 I_{red}(x) := I_{o1} + m_2 \cdot & \left[\begin{aligned} & (7a_{L11} \cdot x^6 + 6a_{L12} \cdot x^5 + 5a_{L13} \cdot x^4 + 4a_{L14} \cdot x^3 + 3a_{L15} \cdot x^2 + 2a_{L16} \cdot x + a_{L17})^2 \dots \\ & + (7a_{\varphi21} \cdot x^6 + 6a_{\varphi22} \cdot x^5 + 5a_{\varphi23} \cdot x^4 + 4a_{\varphi24} \cdot x^3 + 3a_{\varphi25} \cdot x^2 + 2a_{\varphi26} \cdot x + a_{\varphi27}) \cdot \\ & (a_{L11} \cdot x^7 + a_{L12} \cdot x^6 + a_{L13} \cdot x^5 + a_{L14} \cdot x^4 + a_{L15} \cdot x^3 + a_{L16} \cdot x^2 + a_{L17} \cdot x + a_{L18}) \end{aligned} \right] \\
 & + (I_{12} + I_{o3}) \cdot (7a_{\varphi21} \cdot x^6 + 6a_{\varphi22} \cdot x^5 + 5a_{\varphi23} \cdot x^4 + 4a_{\varphi24} \cdot x^3 + 3a_{\varphi25} \cdot x^2 + 2a_{\varphi26} \cdot x + a_{\varphi27})^2
 \end{aligned} \tag{2}$$

Reduced forces are labeled as F_{Pred} appertaining the spring, F_k appertaining the contact and F_{TR} appertaining the damping.

The motion equation solution leads to the output of the coordinate φ_1 - its angular velocity $d\varphi_1$ and φ_1 angle. If the solution failed, it would be necessary to change the solver type (Mathcad "Odesolve" button - ADAMS, FIXED, ...).

The creation of N_t values for the simulation time 0 - tend (φ_1 , $d\varphi_1$, $dd\varphi_1$) is defined with the help of the tt parameter - the time interval vector from 0 to t_{end} divided to N_t values.

6. Contact force simulation results

The resulting contact force - the main goal of the complex tension mechanism simulation is shown in Fig. 6. The contact force peak value of 284.14 N was reached in 0.09 s.

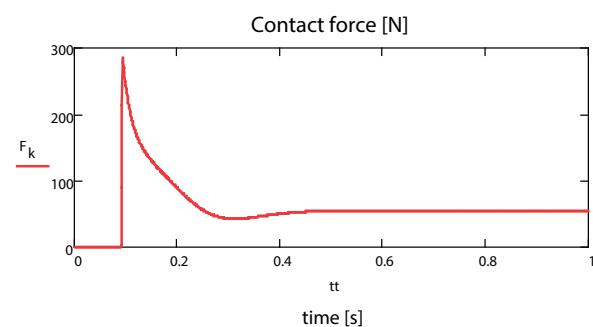


Fig. 6 Tension mechanism contact force calculation result (Source: authors)

7. Conclusion

The mathematical model of the tension mechanism working by a spring motion generation and contacting a rigid body at the end of the motion was built considering the main problem of the analysis - the moment when the mechanism reaches its end position and contacts the frame rigid body with one of its

components. It was necessary to use the right model of the friction and contact properties and to calculate the mechanism coordinates via the interpolation polynomial of the 7-th degree. The result of the simulation was the definition of the peak contact force between the mechanism component and the frame rigid body.

References

- [1] DEKYS, V., BRONCEK, J.: Measuring Strain of the Lattice Towers, *Communications - Scientific Letters of the University of Zilina*, vol. 14, No. 3, 2012, 39-42. ISSN 1335-4205.
- [2] DROZDZIEL, P., KRZYWONOS, L.: The Estimation of the Reliability of the First Daily Diesel Engine Start-up During its Operation in the Vehicle, *Eksplatacja i Niezawodnosc - Maintenance and Reliability* 1(41), 2009, 4-10, ISSN 1507-2711.
- [3] HRCEK, S., KOHAR, R., MEDVECKY, S.: Determination on the Maximum Roller Bearing Load with Regards to Durability there of using FEM Analysis. *Communications - Scientific Letters of the University of Zilina*, vol. 14, No. 3, 2012, 55-61, ISSN 1335-4205.
- [4] HRCEK, S., KRAUS, V., KOHAR, R., MEDVECKY, S., LEHOCKY, P.: Construction of a Bearing Testing Apparatus to Assess Lifetime of Large-scale Bearings. *Communications - Scientific Letters of the University of Zilina*, vol. 11, No. 2, 2009, 57-64, ISSN 1335-4205.
- [5] BRUMERCIK, F., KOCUR, R., PAZICAN, M., LUKAC, M.: Differential Hydro-mechanical Transmissions with Hydrostatic Units. *Communications - Scientific Letters of the University of Zilina*, vol. 7, No. 1, 2005, pp. 49-53, ISSN 1335-4205.
- [6] WU, D., YAO, J., LI, H., QIAN, B.: Control Strategy for Hydro-mechanical Differential Turning System of Tracked Vehicles, *Nongye Gongcheng Xuebao / Transactions of the Chinese Society of Agricultural Engineering*, vol. 28, No. 8, 2012, 78-83, ISSN 1002-6819.
- [7] KOHAR, R., HRCEK, S., MEDVECKY, S.: Usage of Dynamic Analysis to Determine Force Interactions between Components of Rolling Bearings. *Communications - Scientific Letters of the University of Zilina*. vol. 14, No. 3, 2012, 62-67, ISSN 1335-4205.
- [8] KUCERA, L., LUKAC, M., JURAK, L., BRUMERCIK, F.: Hydromechanical Automatic Transmission, *Communications - Scientific Letters of the University of Zilina*, vol. 11, No. 2, 2009, 33-35, ISSN 1335-4205.
- [9] LEHOCKY, P., KOHAR, R., HRCEK, S., PODHORSKY, J., SURMOVA, B., MEDVECKY, S., HRCEKOVA, A.: Automative Unwinding of Waste Paper from Reel Spools. *Communications - Scientific Letters of the University of Zilina*, vol. 9, No. 1, 2007, 60-66, ISSN 1335-4205.
- [10] WANG, G., ZHU, S., SHI, L., TAO, H., VANTHINH, N.: Experimental Optimization on Shift Control of Hydraulic Mechanical Continuously Variable Transmission for Tractor, *Nongye Gongcheng Xuebao / Transactions of the Chinese Society of Agricultural Engineering*, vol. 29, No. 18, 51-59, 2013, ISSN 1002-6819.